robotics

MDPI

Article

Feasibility and Application of the B.E.A.T. Testbed for Assessing the Effects of Lower Limb Exoskeletons on Human Balance

Ilaria Mileti [1,*], Juri Taborri [2,*], David Rodriguez-Cianca [3], Diego Torricelli [3], Stefano Rossi [2] and Fabrizio Patanè [1]

1 Department of Engineering, University Niccolò Cusano, 00166 Rome, Italy
2 Department of Economics Engineering Business Organization (DEIM), University of Tuscia, 01100 Viterbo, Italy
3 Neuralrehabilitation Group of the Spanish National Research Council (CSIC), 28006 Madrid, Spain
* Correspondence: ilaria.mileti@unicusano.it (I.M.); juri.taborri@unitus.it (J.T.)

Abstract: Assessing the performance of exoskeletons in assisting human balance is important for their design process. This study proposes a novel testbed, the B.E.A.T (Balance Evaluation Automated Testbed) to address this aim. We applied the B.E.A.T to evaluate how the presence of a lower limb exoskeleton influenced human balance. The B.E.A.T. consists of a robotic platform, standardized protocols, and performance indicators. Fifteen healthy subjects were enrolled and subjected to repeatable step-type ground perturbations in different directions using the multi-axis robotic platform. Each participant performed three trials, both with and without the exoskeleton (EXO and No-EXO conditions). Nine performance indicators, divided into kinematic and body stability indicators, were computed. The reliability of performance indicators was assessed by computing the Inter Class Correlation (ICC). The indicators showed good ($0.60 \leq$ ICC < 0.75) to excellent (ICC ≥ 0.75) reliability. The comparison between the EXO and No-EXO conditions revealed a significant increase in the joint range of motion and the center of pressure displacement while wearing the exoskeleton. The main differences between the EXO and No-EXO conditions were found in the range of motion of the knee joints, with an increment up to 17° in the sagittal plane.

Keywords: exoskeleton benchmark; motion measurement; robotic platform; reliability; balance assessment; kinematics

Citation: Mileti, I.; Taborri, J.; Rodriguez-Cianca, D.; Torricelli, D.; Rossi, S.; Patanè, F. Feasibility and Application of the B.E.A.T. Testbed for Assessing the Effects of Lower Limb Exoskeletons on Human Balance. *Robotics* **2022**, *11*, 151. https://doi.org/10.3390/robotics11060151

Academic Editor: Dan Zhang

Received: 11 November 2022
Accepted: 13 December 2022
Published: 15 December 2022

1. Introduction

Lower limb exoskeletons and powered orthoses are wearable electromechanical devices developed to enhance, rehabilitate or assist human bipedal performance, e.g., gait [1–3]. Despite the fast-growing exoskeleton market, several technical bottlenecks have prevented their wider application up to now.

One of the main drawbacks of most solutions is the inability to fully fit the users' anatomy, given the rigid mechanical structure [4]. This may lead to a kinematic mismatch between the user and the robot, resulting in movement alterations, early fatigue, and discomfort.

The evaluation of the performance of lower limb exoskeletons in assisting human movement has become an important issue in recent years [5]. To date, several studies investigated the influence of the mechanical design of exoskeletons on motor capabilities with heterogeneous approaches [3]. Some studies proposed the use of an asymmetric parallel mechanism to reduce the effects of mechanical constraints [6]. Other studies focused on how the lack of anatomical degrees of freedom influenced the walking behavior of healthy adults [7]. The results showed that locking the ankle imposed a change in the trajectory of the hip and knee joints. Exoskeletal configuration, with an unlocked anterior–posterior translation at the hip level, reported better performance in terms of shorter adaptation time [8]. Wearing a heavy exoskeleton was shown to alter stride length [9], stride time [10], and step width [11], and to require up to 50 strides for motor adaptation [12]. Moreover, longer linkage misalignment was found to be less critical in terms of human–robot interaction forces in comparison with the same misalignment given by shorter linkage [13].

Despite these results being interesting, an important drawback gleaned from analysis of the literature is the lack of studies investigating the effects of exoskeleton constraints on human kinematics during postural tasks [14,15], in contrast to the high number of experiments with exoskeletons performed during walking conditions. The importance of testing bilateral lower limb exoskeletons in dynamic posturography scenarios lies in the fact that the mechanical design required to assist walking could represent a hazardous constraint in cases of unforeseen balance perturbations. Therefore, the limits on the degrees of freedom imposed by the exoskeleton on the anatomical joints of the hip, knee and ankle, could hamper a subject's postural control strategies. Luger et al. [15] tested the influence of passive lower limb exoskeletons during manual handling tasks, showing that such devices did not significantly influence postural sway in bipedal static stance, and the human center of pressure was unchanged. The effect of a unilateral passive exoskeleton for the knee and ankle joints during standing and dynamic posturography scenarios was evaluated by Ringhof et al. [14]. In dynamic conditions, the time required for participants to regain stability was not affected by the presence of the exoskeleton. However, even though the users were subjected to external perturbations using a typical dynamic posturographic methodology, the dynamics of the center of pressure were not investigated. Although these studies played a key role in the design and improvement of new wearable robots for the lower limbs, the different designs used, the different methodologies, the different protocols, and the different motor conditions of the testbed populations, mean that comparing their results is not viable. In addition, in the majority of the studies, researchers focused on validating an existing exoskeleton design as a whole, without considering the effects of the simple mechanical constraints of the device, which, in turn, are often not very different between one exoskeleton and another. Therefore, it is still unclear whether human postural control strategies are altered when subjected only to the mechanical constraints imposed by the use of an exoskeleton.

In this context, the need to develop reliable and replicable testing methods as the foundation of a standardized benchmarking ecosystem for wearable robots, as demonstrated by several international consortia that target this purpose [16–18], is becoming a fundamental issue. In the rehabilitation field, several methods were developed to assess the postural control strategies of humans in dynamic conditions [19]. Robotic mobile surfaces capable of providing external perturbation of the base of support of the subject are generally the most used tools in dynamic posturography. Commercially available moving platforms are the Equitest [20], Proprio 5000-Dynamic Balance System [21], BalanceQuest [22], and CAREN-Motek Medical [23]. At least one of the following limitations characterizes such devices: inability to provide perturbations on the yaw axis, lack of impedance control, bulky structure, limited measurement, inability to trigger external systems and small base support area.

These shortcomings led to the need to develop a standard testing methodology (procedure and metrics) for assessing the performance of wearable exoskeleton during dynamic posturography, which fulfils the specification of a benchmarking ecosystem. Therefore, this study aimed to overcome the limitations presented in previous studies and to verify the feasibility of using a robotic testbed for the analysis of the effect of an exoskeleton controlled in a transparent mode on human balance. The method consists of a comprehensive Testbed, named B.E.A.T. (Balance Evaluation Automated Testbed) [24]. The testbed consists of the Roto.BiT3D platform, a robotic mobile base capable of providing standardized perturbation profiles, a set of protocols and a set of performance indicators, based on literature study [19].

This study evaluated the feasibility of the use of a robotic testbed, literature metrics, and standardized perturbations to be implemented for performance evaluation of the exoskeleton. Then, we applied the B.E.A.T. protocols to a cohort of healthy subjects wearing a standard-type exoskeleton in order to study the induced effects on postural strategies. In addition to the validation of a new exoskeleton benchmarking methodology, the findings of the present study provide useful information for improving the design of lower limb exoskeletons, taking into account their ability to assist balance.

2. Materials and Methods

2.1. Participants

A cohort of 15 healthy young adults (7 M, 8 F; age: 28 $\pm$ 4 years) was enrolled in this study. Each participant met the following inclusion criteria: absence of neurological or musculoskeletal disorders, vestibular diseases, dizziness, long-term medications, and bone lesions or joint pathologies of the lower limbs and upper body in the year before the study. All the participants had no previous experience of the procedure and equipment. Before being included in the experimental cohort, written informed consent was collected from all participating subjects. The study complied with the principles of the Declaration of Helsinki and the protocol was approved by the Ethical Committee of the Spanish National Research Council (approval number: 091/2021) as part of the H2020 European project EUROBENCH (grant number: 779963).

2.2. Apparatus

The apparatus was composed of the B.E.A.T system, the exoskeleton EXO-H2 and the kinematic measurement system.

2.2.1. The B.E.A.T. System

The B.E.A.T. benchmarking system consists of: (i) a 3-Degress of Freedom (DoF) robotic mobile base, named Roto.Bit3D, with an external frame; (ii) an embedded measurement system; (iii) a set of pre-defined experimental testing protocols that can be carried out with the system; and iv) a set of performance indicators for the assessment of lower limb exoskeleton performance in assisting human balance. The robotic mobile base, named the Roto.BiT3D (v 3.0), is a new version of a 3-DoF parallel robot, the Roto.Bit3D [25] and 1-DoF robot, the Roto.Bit1D [26,27]. The platform has a moving plate with a diameter of 750 mm and an overall height of 365 mm. The workspace allows the motion of the moving plate in a range of $\pm 10^{\circ}$ for roll and pitch angles, whereas it allows $\pm 15^{\circ}$ for yaw angle. The platform is controllable both in position and impedance mode, and provides arbitrary 3-DoF rotations around the roll, pitch, and yaw axes with respect to a fixed point allocated on the center of the base, with a maximum speed of $50^{\circ}/s$. The full scale is 100 kg off-center by 15 cm. As shown in Figure 1a,b, the moving base is connected to three linear actuators through three rigid linkages and six spherical joints. Each of the three arms is equipped with a uni-axial load cell (KM30z, ME-Meßsysteme GmbH, Hennigsdorf, Germany) for the measurement of moment exerted by the subject over the moving plate. In addition, the moving plate is connected to the fixed frame through a spherical joint with a 6-axis load cell (IFF6A40-B, Danetech, Milan, Italy). A pressure matrix (Sensor Medica, Italy, Rome) is embedded into the moving plate for the assessment of pressure distribution, and Center of Pressure (CoP) displacement, see Figure 1c. The pressure matrix has a total area equal to 598×518 mm^2 and is composed of 3000 resistive sensors (50 rows and 60 columns). Each sensor has a sensitive area of 1 cm $\times$ 1 cm. The maximum uncertainty in the measurement of CoP was estimated to be equal to 0.13 cm for calibrated mass and 0.08 cm for tests involving subjects [24]. The sampling frequency of CoP displacement was set at 100 Hz. The robotic mobile base is surrounded by an external frame to guarantee subject safety. The structure is composed of aluminum profiles for an overall mass of 105 kg and dimension 2.6 m $\times$ 1.6 m $\times$ 1.4 m.

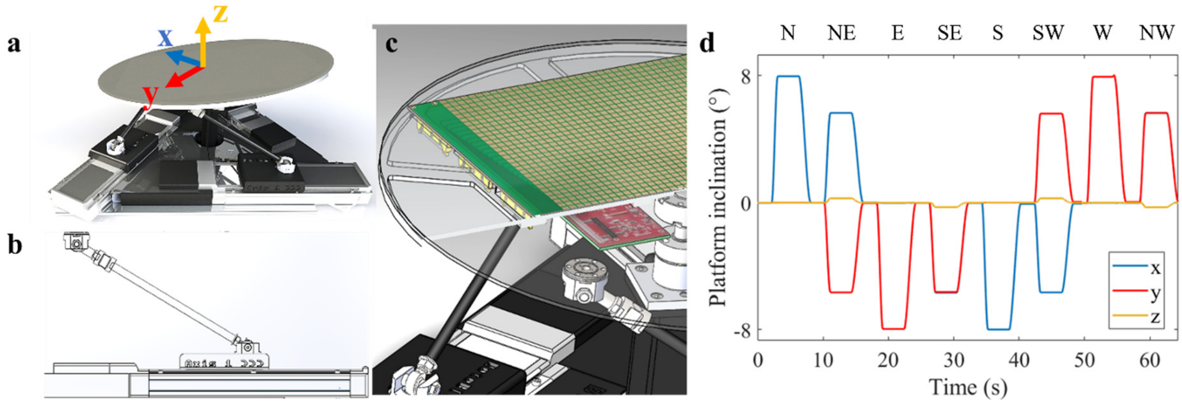

Figure 1. Schematics of the robotic mobile base and overview on the platform rotation over the protocol: (**a**) the moving plate and three linear motors of the Roto.BiT^{3D}, the north direction is directed as the x-axis of the platform coordinate system; (**b**) lateral view of the Roto.BiT^{3D} with the three fixed-length arms connected to the three linear motors; (**c**) overview of the pressure matrix on the moving plate; (**d**) platform inclinations over the three axis.

The control system of the B.E.A.T. offers a set of seven standardized testing protocols for the analysis of the performance of lower limb exoskeletons. Testing protocols can be divided into position and impedance modes. In position control mode, the platform is commanded to reach specific angular positions of the base. In impedance mode, the moving plate simulates a 3D spring/damper system that can be controlled by tuning, for each DoF, stiffness, time constant, and equilibrium angle [25]. Among all the possible testing protocols made available by the B.E.A.T. system, we selected the one named SPe (Step Perturbation Even Surface). The SPe protocol configured the moving base in positional control mode. Eight step perturbations were provided within the protocol, one per direction according to the principal eight cardinal points: north (N), north-east (NE), east (E), south-east (SE), south (S), south-west (SW), west (W), and north-west (NW). Each step involved a descending phase, in which the moving plate was inclined at 8°, and an ascending phase, in which the moving plate returned to the horizontal position for an overall time duration of 8 s per cardinal point, as illustrated in Figure 1d. It should be noted that in the N and S directions, the platform had a tilt of the same magnitude, but opposite sign, along the x-axis (blue line), Figure 1d. For the E and W directions, there was the same tilt, with opposite sign, along the y-axis (red line), while for NE and SW there was an inverted combination of the tilt angle, Figure 1d.

For the analysis of the performance of lower limb exoskeletons in human balance, the B.E.A.T system provided several performance indices based on the embedded sensor system, divided into Body Stability and Response to Perturbation indicators. In this study, three indices were selected from the set of Body Stability indicators to be used in the analysis: Path Length of the Centre of Pressure (CoP), Path length of the Centre of Pressure in the anterior–posterior direction, Path length of the Centre of Pressure in the medial–lateral direction. More details of the analysis of the performance indicators are reported in the Section 2.4.

2.2.2. The EXO-H2

In addition to the B.E.A.T. system, the EXO-H2 was used in the case study, Figure 2. The EXO-H2 is a lower limb exoskeleton conceived for the rehabilitation of stroke patients or patients having spinal cord injuries [28]. In this study, the EXO-H2 was acting as a passive orthosis, as its actuators were decoupled from the structure. In this manner, it was possible to simulate the mechanical constraints of an exoskeleton controlled in a transparent mode. In fact, since no control architecture was implemented, so as to provide a fully transparent mode that was perfectly capable of passively following human movements, all motor shafts were physically decoupled. In this way, the weight of the exoskeleton might be relevant only in particular configurations, such as hip and knee flexion. However, the low velocity intensity of perturbations used in this study and the subject's posture was not such as to produce significant inertial loads. The EXO-H2 consists of a bilateral wearable device with hip, knee, and ankle-powered joints, designed for the overground gait training of adults between 1.50 m and 1.95 m of height (maximum mass of 100 kg). The mechanical frame of EXO-H2 is composed of aluminum uprights for the thighs and the shanks. In addition, the structure is composed of articulated footplates and waist support. The actuated joints and external frame allow passive and active movement in the sagittal plane, with the following range of flexion/extension motion for the hip, knee, and ankle joints, respectively: (+100°, −20°), (+100°, −3°), (+20°, −20°)/ The remaining anatomical DoFS of the lower limbs were theoretically constrained by the rigid structure. However, in practice, due to the exoskeleton's interface compliance and human soft tissue deformation, certain movements in theoretically impossible directions might exist, at least for a limited ROM. The length of the external frame could be adjusted, based on the subject's characteristics, via two telescopic bars. Adjustable rounded leg braces with Velcro straps could be customized to meet individual needs. Users did not feel any extra weight while standing, because the exoskeleton maintained its weight through the mechanical frame. The joint actuators were brushless DC motors (Maxon, EC60 Flat Brushless) coupled to Harmonic Drive gearboxes.

Figure 2. Lateral and frontal views of a subject wearing the H2 exoskeleton with the inertial sensor.

2.2.3. Kinematic Measurement System

It is worth noting that the B.E.A.T. system is able to manage external measurement systems, such as optoelectronic, inertial sensors and electromyography systems, for which additional performance indicators can be computed. In this study, a wearable inertial measurement system was used for the analysis of the presence of the lower limb exoskeleton on lower limb kinematics. Seven Inertial Measurement Units (IMUs) (MTw, Xsens Technologies—Enschede, The Netherland) were used for the analysis of the kinematics of the pelvis, thighs, shanks and feet. Figure 2 shows the sensors' positioning on a participant while wearing the EXO-H2. The sampling frequency was set to 100 Hz.

2.3. Experimental Protocol

The experimental protocol was conducted at the EUROBENCH facility located in the Hospital Los Madroños, Madrid (Spain). Participants underwent a training session with the Roto.BiT3D to give them an initial experience of the moving plate, and for familiarization with the testing protocol. The training session lasted until the participant felt familiar with the equipment and the platform motion. The experimentation consisted of one session named No-EXO condition (No-EXO) and one session named EXO condition (EXO). In the No-EXO condition, participants were required to perform the SPe protocol without wearing the exoskeleton. In the EXO condition, participants performed the SPe protocol wearing the EXO-H2. Before each session, participants performed a Functional Calibration procedure advised by an operator, which was necessary for IMU kinematic tracking. The Functional Calibration procedure provided sensor orientations with respect to body segment, to complete the body-to-sensor alignment procedure and to gather joint angles in the anatomical plane [29]. Afterwards, participants were asked to maintain their balance while standing in an upright position over the moving platform. In the initial position, subjects stood on the platform with feet symmetrically placed at the center of rotation of the moving base, shoulder width apart. To guarantee the same initial condition, and to assure a consistent position of participants within and across trial blocks, subjects were asked to adjust their feet position till their CoP was close to the center of the moving base. In addition, participants were instructed to keep their eyes open and to gaze at a fixed point at eye level for the entire session [30]. During the protocol, participants were asked to simply maintain balance, avoiding any steps on the foot support, and avoiding excessive arm movements. The trial did not start until subjects declared themselves ready to begin; moreover, a verbal warning was given before the trial started. The SPe testing protocol was repeated three times for each condition (No-EXO and EXO). Thus, an overall of six trials was performed. The order of conditions and the order of trials was randomized across subjects in order to avoid bias on the results due to trial order. Between the trials, a time interval of at least 20 s was set to allow free motion of the participant on the still platform. The whole experimentation, comprehensive of equipment phase, familiarization and testing protocols, lasted not more than 30 min per participant.

2.4. Data Analysis

Data were analyzed offline with Matlab (2021a, MathWorks, Natick, MA, USA). For the assessment of postural strategies, a set of four performance indicators was selected. The performance indicators were divided into two main categories: body stability and kinematics. For the body stability category, three performance indicators were selected: (i) mean value across trials of the Path Length of the Center of Pressure (PL); (ii) mean value across trials of the Path length of the Center of Pressure in anterior–posterior direction (PL_{AP}); and in the medial–lateral direction (PL_{ML}). The coordinates of the CoP were computed by the B.E.A.T. software as follows:

$$\mathrm{CoP}_x = \frac{1}{\sum_{\mathrm{k}}^{\mathrm{N}} \mathrm{P_k A_k}} \left[\sum_{\mathrm{k}}^{\mathrm{N}} \mathrm{P_k A_k x_k}\right] \tag{1}$$

$$\mathrm{CoP}_y = \frac{1}{\sum_{\mathrm{k}}^{\mathrm{N}} \mathrm{P_k A_k}} \left[\sum_{\mathrm{k}}^{\mathrm{N}} \mathrm{P_k A_k y_k}\right] \tag{2}$$

where (x_k, y_k) are the coordinates of the position of the k-th sensor in the pressure matrix, P_k is the pressure at the k-th sensor and A_k is the area of the k-th sensor. Each sensor had an acquisition frequency of 100 Hz. The pressures of each sensor were digitally converted to integer values between 0 and 255.

More details on the computation of CoP components in the horizontal plane are reported in [30]. The PL represents the distance covered by the Center of Pressure (CoP) in the horizontal plane, according to the following formula:

$$\mathrm{PL} = \sum_{\mathrm{n}=1}^{\mathrm{N}-1} \left[(\mathrm{AP[n+1]} - \mathrm{AP[n]})^2 + (\mathrm{ML[n+1]} - \mathrm{ML[n]})^2\right]^{1/2} \tag{3}$$

where AP and ML are the anterior–posterior and medial–lateral components of the CoP, while n represents the number of points during the task. Equation (3) was used for the computation of PL_{AP} and PL_{ML} by considering the ML and AP components equal to zero, respectively. All the body stability indicators were computed separately over the above-mentioned eight perturbation directions, during the descending phase of the mobile base.

The estimation of kinematic parameters was performed by modeling lower limbs as seven body segments bj = 1 . . . 7 (pelvis, right and left thigh, right and left shank and right and left foot) connected through six spherical joints (right and left hip, right and left knee and right and left ankle). More details of the angle joint computation are reported in [28]. For the kinematics, the Range of Motion (ROM) was evaluated for each angle joint in the sagittal plane and separately for all the perturbation directions. The mean value of the range of motion of all participants was computed over the three trials, separately for all the eight cardinal perturbation directions: north (ROMN), north-east (ROMNE), east (ROME), south-east (ROMSE), south (ROMS), south-west (ROMSW), west (ROMW), and north-west (ROMNW).

It is worth noting that all the performance indicators were not influenced by the test duration, since the duration of the SPe protocol was fixed to 64 s and all the directions had the same duration.

A scheme of the experimental set-up, experimental protocol and performance indicators is provided in Figure 3.

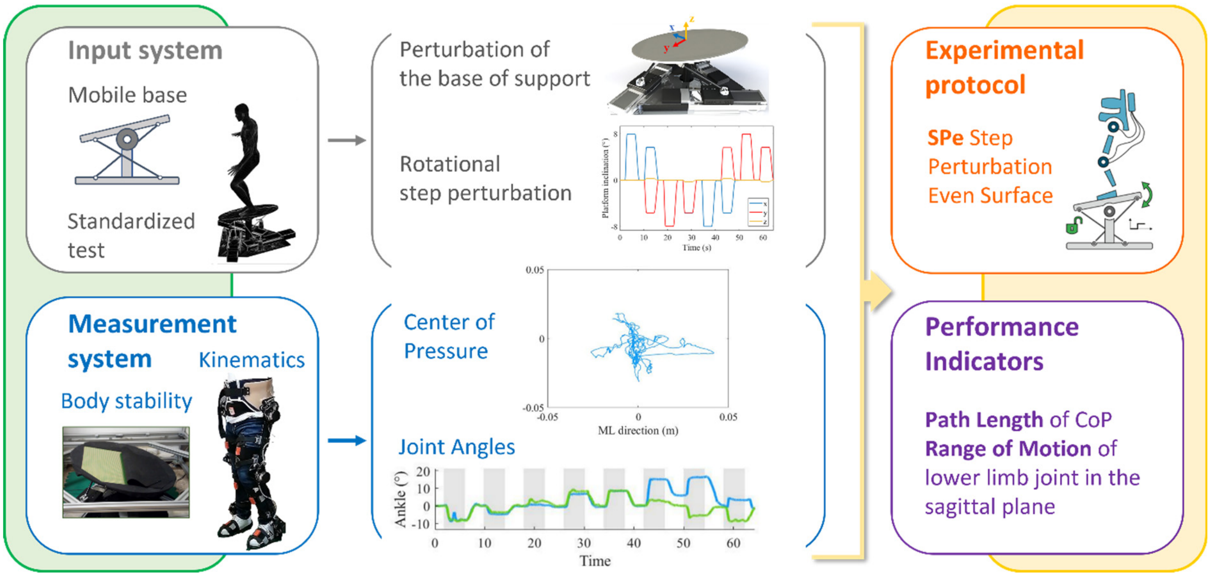

Figure 3. Schematics of the B.E.A.T. benchmarking system.

2.5. Statistical Analysis

Statistical analysis was performed with the SPSS package (IBM-SPSS Inc., Armonk, NY, USA) and all data were tested for normality by means of the Shapiro–Wilk test.

To verify the feasibility of using the proposed performance indicators, the reliability was analyzed. Reliability was assessed with the Intraclass Correlation Coefficient (ICC) with an ICC (2,1) model. Reliability was classified as excellent (ICC $\geq$ 0.75), good (0.60 $\leq$ ICC < 0.75), fair (0.40 $\leq$ ICC < 0.60), and poor (0.00 $\leq$ ICC < 0.40), in accordance with [31].

For the assessment of exoskeleton effects on postural strategies, a two-way repeated measures ANOVA test was applied, with Directions (eight levels: north, north-east, east, south-east, south, south-west, west, north-west) and conditions (two levels: Exo and No-Exo) as within-subject factors. When significant differences were found, a multiple comparison Bonferroni's test was performed. The Greenhouse–Geisser correction was adopted when the Mauchly's test was significant and the assumption of sphericity was violated. Otherwise, the p-value of sphericity was considered. If the interaction effect Directions $\times$ Conditions was significant, the two-way repeated measures ANOVA was broken down, comparing Exo and No-Exo separately. More specifically, a one-way repeated measures ANOVA with Directions (eight levels) was performed for the No-EXO and the

EXO conditions. Furthermore, comparisons between conditions were performed by a paired Student's *t*-Test for each direction.

For all the tests, the statistical significance was set at 0.05.

3. Results

3.1. Feasibility of the Performance Indicators

As regards the test–retest reliability, the ICC values for the mROM of all the joint angles, along with PL, PL_{AP} and PL_{ML} in the overall directions, are reported in Table 1.

Table 1. Inter-Class Coefficient for the Performance indicators: Range of Motion (ROM) of the lower limb joint angles, for both the right (R) and left (L) side; the overall Path length of the Center of Pressure (PL); the Path length in the medial-lateral (PL_{ML}) direction and the Path length in the anterior-posterior (PL_{AP}) direction of the Center of Pressure. ICC values are reported for all the perturbations direction in the No-Exo. The ICC values in the range of ICC $\geq$ 0.75 and 0.60 $\leq$ ICC < 0.75, are reported in dark and light green, respectively.

	N	**NE**	**E**	**SE**	**S**	**SW**	**W**	**NW**
ROM of Joint Angles								
Left								
Hip	0.91	0.95	0.96	0.96	0.97	0.97	0.98	0.78
Knee	0.93	0.97	0.98	0.95	0.94	0.99	0.99	0.86
Ankle	0.84	0.97	0.97	0.94	0.91	0.99	0.96	0.65
Right								
Hip	0.91	0.97	0.97	0.80	0.93	0.98	0.94	0.96
Knee	0.92	0.99	0.99	0.79	0.97	0.95	0.96	0.99
Ankle	0.86	0.95	0.98	0.81	0.93	0.93	0.95	0.94
CoP								
PL	0.69	0.93	0.95	0.94	0.89	0.96	0.95	0.94
PL_{ML}	0.75	0.94	0.94	0.94	0.92	0.96	0.95	0.95
PL_{AP}	0.68	0.90	0.82	0.91	0.85	0.91	0.84	0.90

In the No-EXO condition, kinematic indices reported excellent reliability ICC $\geq$ 0.75, except for the range of motion of the left joint ankle, which reported an ICC value in the range of 0.60 $\leq$ ICC < 0.75 in the NW direction. For the body stability, excellent reliability was observed for all the indicators, except for the overall path length and the path length in the medial-lateral direction in the north condition that reported good ICC values.

3.2. Case Study: Influence of Exoskeleton Mechanical Constraints on the Postural Strategies

Mean and standard deviation of performance indicators value in all the perturbation directions are reported in Table 2. Lower limb joint angles in the sagittal plane of one subject in the No-EXO and EXO conditions are reported in Figure 4. The statokinesigrams of the same participant are reported in Figure 5. Results of the two-way repeated measure ANOVA reported significant interactions between the two variables, Directions $\times$ Conditions, for all the statistical analyses related to the kinematic and body stability performance indicators. The *p*-values of the interaction effects of the kinematic PI were lower than 0.01 for the range of motion of left joints and <0.01, 0.02, <0.01 for the range of motion of the hip, knee and ankle of the right side, respectively.

As regards the body stability performance indicators, *p*-values of the interaction effects were: <0.01, 0.02, <0.01 for PL, PL_{ML} and PL_{AP}, respectively. Since the interaction effects were statistically significant in all the performance indicators, each two-way repeated measure ANOVA was broken down into two one-way repeated ANOVA measurements, one for each Equipment Condition, No-EXO and EXO, and into eight paired *t*-tests, one per perturbation direction. Table 3 reports the mean and standard deviation values of the performance indicators for all the perturbation directions.

Table 2. Mean and standard deviation of performance indicators value in all the perturbation directions. Significance between non-equipped and equipped condition with H2 are starred: * indicates a p-values < 0.05; and ** indicates a p-values < 0.01.

			N	NE	E	SE	S	SW	W	NW
Joint Angle (°)										
L	Hip	No-EXO	1.8 ± 0.9	4.8 ± 4.2 *	6.2 ± 4.8 **	4.5 ± 3.9 **	2.7 ± 2.2	5.1 ± 5.5	5.1 ± 6.6	3.2 ± 2.4
		EXO	1.9 ± 1.0	10.3 ± 7.3	15.2 ± 6.0	12.1 ± 6.1	1.9 ± 0.8	2.3 ± 1.7	4.6 ± 2.5	4.8 ± 1.6
	Knee	No-EXO	2.8 ± 3.7	7.0 ± 8.7 *	9.5 ± 10.4 **	7.2 ± 8.8 **	2.8 ± 2.9	6.3 ± 10.9	6.7 ± 12.6	3.6 ± 4.1
		EXO	1.8 ± 1.1	16.2 ± 13.7	26.4 ± 10.6	23.1 ± 10.2	2.1 ± 1.4	2.3 ± 1.0	2.7 ± 1.4	2.9 ± 1.3
	Ankle	No-EXO	8.6 ± 1.9	5.5 ± 1.9	5.9 ± 5.5 **	10.1 ± 4.9 **	9.8 ± 1.9	6.4 ± 5.2	5.0 ± 4.6	8.4 ± 0.6
		EXO	7.2 ± 2.2	6.8 ± 4.6	16.0 ± 4.0	18.3 ± 4.4	8.0 ± 2.2	3.1 ± 2.2	5.1 ± 1.7	7.5 ± 2.1
R	Hip	No-EXO	1.9 ± 1.2	4.4 ± 5.7	4.9 ± 6.2	4.2 ± 4.1	2.5 ± 1.3	7.4 ± 6.0	8.8 ± 7.0	10.8 ± 6.1
		EXO	2.5 ± 2.7	3.4 ± 1.2	4.0 ± 1.8	2.8 ± 1.3	2.0 ± 1.8	11.6 ± 4.4	14.9 ± 5.2	12.5 ± 4.9
	Knee	No-EXO	3.0 ± 4.0	6.5 ± 11.6	7.0 ± 11.7	4.9 ± 7.2	2.7 ± 1.6	10.4 ± 12.9 **	13.1 ± 14.3 **	10.8 ± 13.3 **
		EXO	3.0 ± 3.7	2.5 ± 1.6	2.1 ± 0.9	1.5 ± 0.4	2.7 ± 2.4	23.5 ± 10.0	30.4 ± 9.6	24.6 ± 10.2
	Ankle	No-EXO	6.9 ± 2.8	6.3 ± 4.1	6.4 ± 6.1	8.9 ± 4.1	8.1 ± 2.7	7.9 ± 6.3**	7.2 ± 4.1 **	7.7 ± 2.8
		EXO	7.6 ± 2.3	5.8 ± 1.7	3.3 ± 2.7	7.0 ± 2.3	9.9 ± 1.9	16.9 ± 5.9	14.7 ± 4.5	8.3 ± 2.7
CoP (cm)										
	PL	No-EXO	7.9 ± 3.5	7.7 ± 3.5	7.8 ± 2.3 **	7.2 ± 1.3 *	6.9 ± 0.9 **	8.5 ± 2.0	8.4 ± 2.9	7.0 ± 2.1 *
		EXO	7.0 ± 1.9	10.0 ± 2.6	13.2 ± 3.5	11.5 ± 3.4	9.1 ± 1.9	10.8 ± 2.6	10.2 ± 2.8	9.0 ± 1.6
	PL_{ML}	No-EXO	4.8 ± 1.4	5.6 ± 2.2	6.2 ± 2.0 **	5.5 ± 1.2 *	4.6 ± 0.5 *	6.7 ± 2.2	7.0 ± 2.6	5.3 ± 1.6 *
		EXO	4.7 ± 1.2	8.0 ± 2.0	11.1 ± 3.2	8.8 ± 2.8	6.1 ± 1.7	8.6 ± 2.7	8.5 ± 2.9	7.0 ± 1.9
	PL_{AP}	No-EXO	5.1 ± 3.1	4.2 ± 2.5	3.7 ± 1.2 *	3.6 ± 0.8 *	4.1 ± 0.9 *	3.8 ± 1.0 *	3.4 ± 1.1	3.5 ± 1.3
		EXO	4.1 ± 1.3	4.5 ± 1.2	5.0 ± 1.5	5.8 ± 1.5	5.3 ± 0.6	5.0 ± 0.8	4.0 ± 0.8	4.3 ± 0.9

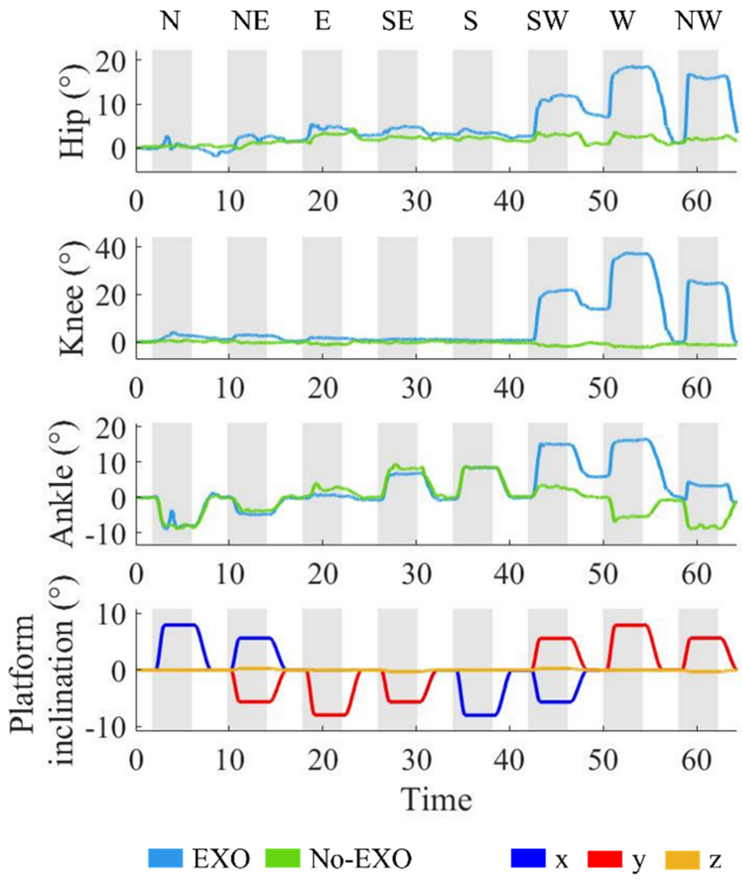

Figure 4. Lower limb joint angles in the sagittal plane of the right side of one participant in the No-EXO (green lines) and EXO (blue lines) conditions and platform inclination over the entire SPe testing protocol. The north direction is directed as the x-axis of the platform coordinate system.

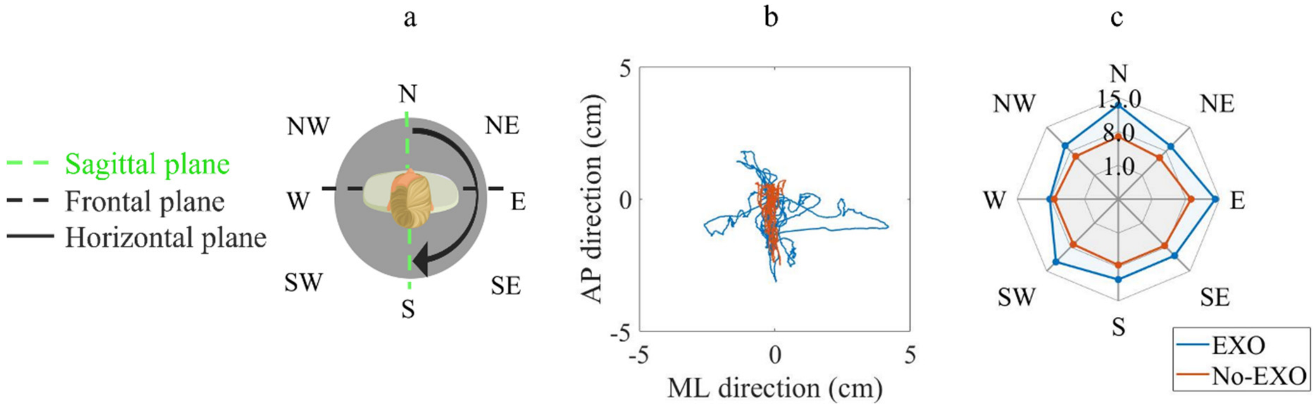

Figure 5. Centre of Pressure (CoP) displacement of a participant: (**a**) schematics of the top view of the participant over the mobile base (the plane free to exoskeleton constraints is reported in green); (**b**) CoP trajectory during the entire duration of the SPe testing protocol in the No-EXO (red line) and EXO (blue line) conditions; (**c**) path length (PL) of the same participant in all cardinal points, expressed in cm.

Table 3. Statistical analysis of repeated measure ANOVA: point and triangle refer to statistical differences in the EXO and No-EXO conditions, respectively. Legend of colors and shapes is reported in Table 4.

	EXO								No-EXO							
	N	**NE**	**E**	**SE**	**S**	**SW**	**W**	**NW**	**N**	**NE**	**E**	**SE**	**S**	**SW**	**W**	**NW**
N		red● orange● black● grey●	red● orange● magenta● black● grey●	red● orange● magenta● black● grey●	cyan● black● ○	blue● green● cyan● black● grey●	blue● green● cyan● black● grey●	blue● green● black● grey●			red▲	red▲		magenta▲	blue▲ grey▲	
NE	red● orange● black● grey●		magenta● black● grey●	magenta●	orange● cyan● grey●	orange● blue● green● cyan●	orange● blue● green● cyan●	orange● blue● green●							blue▲ grey▲	
E	red● orange● magenta● black● grey●	magenta● black● grey●		red● magenta● black● grey●	red● orange● cyan● black● grey●	red● orange● magenta● blue● green● cyan●	red● orange● magenta● blue● green● cyan●	red● orange● magenta● blue● green● black● grey●	red▲			cyan▲				
SE	red● orange● magenta● black● grey●	magenta●	red● magenta● black● grey●		red● orange● magenta● cyan● black● grey●	red● orange● magenta● blue● green● cyan●	red● orange● magenta● blue● green● cyan●	red● orange● magenta● blue● green●	red▲		cyan▲		red▲ △	black▲	magenta▲ grey▲	
S	cyan● black● ○	red● orange● cyan● grey●	orange● magenta● cyan● black● grey●	red● orange● magenta● cyan● black● grey●		magenta● blue● green● cyan● black● grey●	blue● green● black● grey●	blue● green●				red▲ △		magenta▲	magenta▲ grey▲ △	
SW	blue● green● cyan● black● grey●	red● blue● green● cyan●	red● orange● magenta● blue● green● cyan●	red● orange● magenta● blue● green● cyan●	orange● blue● green● cyan● black● grey●		blue● green● ○	cyan● black● ○	magenta▲			black▲	magenta▲			
W	blue● green● cyan● black● grey●	red● orange● blue● green● cyan●	red● orange● magenta● blue● green● cyan●	red● orange● magenta● blue● green● cyan●	blue● green● black● grey● ○	blue● green●		magenta● cyan● black● grey●	blue▲ grey▲	blue▲ grey▲		magenta▲ grey▲	magenta▲ grey▲ △			magenta▲ blue▲ grey▲
NW	blue● green● black● grey●	red● orange● blue● green●	red● orange● magenta● blue● green● black● grey●	red● orange● magenta● blue● green●	blue● green● ○	green● cyan● black●	magenta● cyan● black● grey●								magenta▲ blue▲ grey▲	

Table 4. Legend of colors and shapes related to Table 3.

Legend	**ROM**			**CoP**		
	Hip	**Knee**	**Ankle**	**PL**	**PL_{ML}**	**PL_{AP}**
Left	red▲ red●	orange▲ orange●	magenta▲ magenta●	black▲ black●	grey▲ grey●	△ ○
Right	blue▲ blue●	green▲ green●	cyan▲ cyan●			

In regard to the range of motion of the left limb, significant differences were found between the No-EXO and EXO conditions when the perturbations elicited the right side of the subject. More specifically, the range of motion of the left knee and hip joint were found to be statistically higher in the EXO condition in the NE, E, SE directions while the range of motion of the left ankle was higher in the E and SE directions. In accordance with the left side, the right side reported higher values of the range of motion of the knee joint in the SW, W, and NW directions, whereas the range of motion of the ankle joint was higher in the SW and W directions. For the body stability indicators, the statistical differences between the two conditions were mainly found in the E, SE and S directions. However, statistically significant differences were observed also in the NW directions for all the PL and PL_{ML} indices.

Table 3 reports the statistical differences among all the perturbation directions, separately for No-EXO and EXO conditions. The results revealed that in the No-EXO condition, the number of statistical differences among directions was lower. In the EXO condition, differences among directions were observed in both the kinematic and body stability indicators. More specifically, range of motion of the joint angles of the left side were greater, especially in the E and SE, than in the other directions. Similarly, for the right side, greater amount of motion was observed in the SW, W and NW directions compared to the others. Concerning the body stability indicators, the N direction reported the higher number of differences with other directions for the overall path length of the CoP and for the path length in the medial–lateral direction.

4. Discussion

4.1. Feasibility of the Performance Indicators

The outcomes of the inter-class correlation coefficient allowed us to affirm that all the performance indicators expressed excellent reliability, regardless of the type, i.e., kinematic or posturographic parameters, and regardless of the examined direction. The results recommended caution only when considering the ankle ROM in the NW direction and the path length in the plane and in AP when focusing on the N direction, due to an ICC value lower than 0.70. The excellent reliability allowed us to assess that the selected indices were not influenced by intra-subject variability in the postural behavior. Similar to other literature studies [32–36], our results confirmed the goodness of indicators based on joint angles and center of pressure displacement, even in the case when subjects were exposed to postural disturbances induced by the B.E.A.T. system. As a conclusion, the proposed indicators could be considered robust with respect to the intra-subject postural response variability. Any potential differences occurred when comparing different subjects or different external robotic devices and could be ascribed to the mechanical design of the robots.

4.2. Case study: Influence of Exoskeleton Mechanical Constraints on the Postural Strategies

By focusing on both the graph of Figure 4, and the outcomes related to the kinematic response, it is observable that only the ankle joint was involved in the reaction to external perturbations in the case of exoskeleton absence, regardless of the perturbation directions. Thus, it was reasonable to deduce that young adults are able to recover after a perturbation of the support base only by adopting an ankle strategy. In fact, the ankle strategy is characterized by a non-negligible range of motion of the ankle and minimal movements of the superior joints of the biomechanical chain [34]. Such a result affirmed that, in the absence of an exoskeleton, the subjects were able to exert sufficient torque in contact with the support surface, ensuring that the hip and the ankle joint movements were not affected by the external perturbation [37]. The outcomes were in line with the literature. It is well known that ankle strategy is adopted in cases of slow and low amplitude perturbations, like the ones provided during the proposed experimental protocol [38]. The statistical differences found between the No-EXO and EXO conditions permitted the assessment that the presence of the H2 exoskeleton did not allow subjects to absorb perturbation, which was, instead, propagated in the superior joints. Thus, we affirmed that the kinematic constraints provided by the exoskeleton had a significant impact on the postural strategy adopted by the subjects. Similar results were found by Fasola and colleagues [39], who reported significant increments of the knee flexion when wearing a locked-ankle passive exoskeleton. In addition, the presence of differences only in medial–lateral and mixed directions, rather than in the anterior–posterior ones, could be ascribed to more difficulties being encountered by the central nervous system when reacting to ML perturbation, as observed in [40], as well as to the constraints imposed by EXO-H2 that allowed free movement only in the sagittal plane. Finally, the differences found on the right side when the perturbation was provided in the left direction and vice versa could be ascribed to the ability of young adults to respond to external perturbations by compensating with the contralateral leg without changing the patterns of the ipsilateral side [41]. Thus, based on the results obtained from the present study, it might be assumed that sagittal DoFs of the hip, knee, and ankle may be sufficient for exoskeletons subject to perturbations only in the sagittal plane (see Table 2, where there were no significant differences between exo/no-exo in the north and south directions). In natural environments, or when walking on uneven terrain, exoskeletons should be designed to include DoFs in the medial–lateral plane in the ankle and hip joints. Otherwise, subjects have to adopt compensatory strategies (generally by flexing the knee joint more) that prevent a healthy gait.

By moving to the analysis of the center of pressure, it was evident how the presence of H2 generally caused an increment of the path length in all the perturbation directions; thus, it could be assessed that the exoskeleton led to greater instability of the subject. This result confirmed that kinematic constraints of the lower limbs can influence dynamic stability during standing position in healthy young subjects [38]. Greater instability could also be ascribed to the role of the knee joint and, more specifically, to the necessity to bend the knee when wearing the exoskeleton (Table 3). It was shown that greater stability was assured when the knee was fully extended since it guaranteed a more vertical alignment of the trunk relative to the base of support, leading to an increase of the compression forces applied on the tibiofemoral joint, one of the main actors in reducing body sway [42].

Focusing on No-EXO, the statistical differences confirmed that the postural strategy adopted by healthy young adults were strongly dependent on the perturbation direction, even when no mechanical constraints were imposed on the subject; in fact, such findings were in line with the differences found during the execution of the star excursion balance test (SEBT) [43]. This direction dependence might also be due to the configuration of the lower extremity, which, in the sagittal plane, resembled a multi-segment inverted pendulum, which was not consistent in medial–lateral perturbations [44]. In addition to the above-mentioned implications, our findings also led to the conclusion that the direction dependence of the balance control in the standing position was even more evident in the presence of kinematic constraints of the lower limb. Even if comparison with previous study was not possible, such a result could be ascribed to previously discussed variations of the physiological kinematic and posturographic patterns in the presence of external perturbations. All the above-reported results should be taken into account when seeking to implement a control system for an exoskeleton assisting human balance, in order to compensate both the kinematic constraint influences and the different responses based on perturbation directions.

It is worth noting that the experiments were conducted when the participants were standing still, and that the rotational perturbations were provided only at the base of the support. In future studies, other tests should be performed during different walking activities in order to effectively evaluate other factors, such as, for example, joint mass and joint compliance [45].

5. Conclusions

In this study, standardized rotational perturbations were provided by a parallel robot, to assess the feasibility of the testbed method and for the analysis of the effects of a paradigmatic lower limb exoskeleton on human motion. The main results demonstrated the feasibility of using the B.E.A.T system and its performance indicators. The performance indicators reported good to excellent levels of reliability. The results of the preliminary analysis of the effects of a lower limb exoskeleton on human balance showed differences in the two conditions, EXO and No-EXO, depending on the direction of the perturbation. In addition, the movement of the knee joint in the sagittal plane seemed to be the most affected by the kinematic constraints imposed by the exoskeleton.

The present study did not consider the effect of kinematic constraints and masses separately. However, it could reasonably be assumed that the main effect was due to the former, as the overall oscillations reduced, causing low inertia and unloaded weight results.

For completeness, the study reports some limitations: the type of perturbations that were potentially learned after the first exposure to the test did not consider translational perturbations given the mechanical nature of the testbed.

Future developments will aim at testing different types of external perturbations and at evaluating a larger number of performance indicators to get a wider perspective on the effects of the mechanical constraints that an exoskeleton imposes on human balance.

Author Contributions: Conceptualization, I.M., J.T., D.R.-C., F.P., S.R. and D.T.; methodology, F.P., S.R., I.M. and J.T.; software, F.P.; investigation, I.M., J.T. and D.R.-C.; resources, F.P., S.R. and D.T.; data curation, I.M.; writing—original draft preparation, I.M. and J.T.; writing—review and editing, D.R.-C., F.P., S.R. and D.T.; supervision, F.P., S.R. and D.T.; funding acquisition, F.P. All authors have read and agreed to the published version of the manuscript.

Funding: This research was funded by the Project EUROBENCH (grant agreement N° 779963, PI: Fabrizio Patanè).

Data Availability Statement: Not applicable.

Acknowledgments: The authors would like to acknowledge Project EUROBENCH for the financial support to this study and the Hospital los Madroños, M-501, Km 17, 900, 28690 Brunete, Madrid, Spain.

Conflicts of Interest: The authors declare no conflict of interest.

References

1. Dollar, A.M.; Herr, H. Lower Extremity Exoskeletons and Active Orthoses: Challenges and State-of-the-Art. *IEEE Trans. Robot.* **2008**, *24*, 144–158. [CrossRef]
2. Cardona, M.; Destarac, M.; Cena, C.G. Robotics for Rehabilitation: A State of the Art. In *Exoskeleton Robots for Rehabilitation and Healthcare Devices*; SpringerBriefs in Applied Sciences and Technology; Springer: Singapore, 2020; pp. 1–11. [CrossRef]
3. Shi, D.; Zhang, W.; Zhang, W.; Ding, X. A Review on Lower Limb Rehabilitation Exoskeleton Robots. *Chin. J. Mech. Eng.* **2019**, *32*, 1–11. [CrossRef]
4. Gálvez-Zúñiga, M.A.; Aceves-López, A. A Review on Compliant Joint Mechanisms for Lower Limb Exoskeletons. *J. Robot.* **2016**, *2016*, 5751391. [CrossRef]
5. Torricelli, D.; Rodriguez-Guerrero, C.; Veneman, J.F.; Crea, S.; Briem, K.; Lenggenhager, B.; Beckerle, P. Benchmarking Wearable Robots: Challenges and Recommendations from Functional, User Experience, and Methodological Perspectives. *Front. Robot. AI* **2020**, *7*, 561774. [CrossRef] [PubMed]
6. Zhang, W.; Zhang, W.; Shi, D.; Ding, X. Design of hip joint assistant asymmetric parallel mechanism and optimization of singularity-free workspace. *Mech. Mach. Theory* **2018**, *122*, 389–403. [CrossRef]
7. Olivier, J.; Ortlieb, A.; Bertusi, P.; Vouga, T.; Bouri, M.; Bleuler, H. Impact of ankle locking on gait implications for the design of hip and knee exoskeletons. In Proceedings of the 2015 IEEE International Conference on Rehabilitation Robotics (ICORR), Singapore, 11–14 August 2015; pp. 618–622. [CrossRef]
8. Stegall, P.; Winfree, K.; Zanotto, D.; Agrawal, S.K. Rehabilitation exoskeleton design: Exploring the effect of the anterior lunge degree of freedom. *IEEE Trans. Robot.* **2013**, *29*, 838–846. [CrossRef]
9. Browning, R.C.; Modica, J.R.; Kram, R.; Goswami, A. The effects of adding mass to the legs on the energetics and biomechanics of walking. *Med. Sci. Sports Exerc.* **2007**, *39*, 515–525. [CrossRef]
10. De Witt, J.K.; Hagan, R.D.; Cromwell, R.L. The effect of increasing inertia upon vertical ground reaction forces and temporal kinematics during locomotion. *J. Exp. Biol.* **2008**, *211*, 1087–1092. [CrossRef]
11. Pennycott, A.; Wyss, D.; Vallery, H.; Riener, R. Effects of added inertia and body weight support on lateral balance control during walking. *IEEE Int. Conf. Rehabil. Robot.* **2011**, *2011*, 5975415. [CrossRef]

12. Noble, J.W.; Prentice, S.D. Adaptation to unilateral change in lower limb mechanical properties during human walking. *Exp. Brain Res.* **2005**, *169*, 482–495. [CrossRef]
13. Zanotto, D.; Akiyama, Y.; Stegall, P.; Agrawal, S.K. Knee Joint Misalignment in Exoskeletons for the Lower Extremities: Effects on User's Gait. *IEEE Trans. Robot.* **2015**, *31*, 978–987. [CrossRef]
14. Ringhof, S.; Patzer, I.; Beil, J.; Asfour, T.; Stein, T. Does a Passive Unilateral Lower Limb Exoskeleton Affect Human Static and Dynamic Balance Control? *Front. Sports Act Living* **2019**, *1*, 22. [CrossRef] [PubMed]
15. Luger, T.; Seibt, R.; Cobb, T.J.; Rieger, M.A.; Steinhilber, B. Influence of a passive lower-limb exoskeleton during simulated industrial work tasks on physical load, upper body posture, postural control and discomfort. *Appl. Ergon.* **2019**, *80*, 152–160. [CrossRef]
16. Bessler, J.; Schaake, L.; Bidard, C.; Buurke, J.H.; Lassen, A.E.B.; Nielsen, K.; Saenz, J.; Vicentini, F. COVR—Towards Simplified Evaluation and Validation of Collaborative Robotics Applications Across a Wide Range of Domains Based on Robot Safety Skills. *Biosyst. Biorobotics* **2018**, *22*, 123–126. [CrossRef]
17. Torricelli, D.; Pons, J.L. EUROBENCH: Preparing Robots for the Real World. *Biosyst. Biorobotics* **2018**, *22*, 375–378. [CrossRef]
18. COST ACTION CA16116 WEARABLE ROBOTS FOR AUGMENTATION, ASSISTANCE OR SUBSTITUTION OF HUMAN MOTOR FUNCTIONS | Jan F Veneman | 5 Updates | 1 Publications | Research Project. Available online: https://www.researchgate.net/project/COST-Action-CA16116-Wearable-Robots-for-Augmentation-Assistance-or-Substitution-of-Human-Motor-Functions (accessed on 12 October 2021).
19. Zampogna, A.; Mileti, I.; Palermo, E.; Celletti, C.; Paoloni, M.; Manoni, A.; Mazzetta, I.; Costa, G.D.; Pérez-López, C.; Camerota, F.; et al. Fifteen Years of Wireless Sensors for Balance Assessment in Neurological Disorders. *Sensors* **2020**, *20*, 3247. [CrossRef] [PubMed]
20. Ferber-Viart, C.; Ionescu, E.; Morlet, T.; Froehlich, P.; Dubreuil, C. Balance in healthy individuals assessed with Equitest: Maturation and normative data for children and young adults. *Int. J. Pediatr. Otorhinolaryngol.* **2007**, *71*, 1041–1046. [CrossRef] [PubMed]
21. Broglio, S.P.; Sosnoff, J.J.; Rosengren, K.S.; McShane, K. A Comparison of Balance Performance: Computerized Dynamic Posturography and a Random Motion Platform. *Arch. Phys. Med. Rehabil.* **2009**, *90*, 145–150. [CrossRef]
22. Ionescu, E.; Morlet, T.; Froehlich, P.; Ferber-Viart, C. Vestibular assessment with Balance Quest: Normative data for children and young adults. *Int. J. Pediatr. Otorhinolaryngol.* **2006**, *70*, 1457–1465. [CrossRef]
23. Lees, A.; Vanrenterghem, J.; Barton, G.; Lake, M. Kinematic response characteristics of the CAREN moving platform system for use in posture and balance research. *Med. Eng. Phys.* **2007**, *29*, 629–635. [CrossRef]
24. Taborri, J.; Salvatori, S.; Mariani, G.; Rossi, S.; Patane, F. BEAT: Balance Evaluation Automated Testbed for the standardization of balance assessment in human wearing exoskeleton. In Proceedings of the 2020 IEEE International Workshop on Metrology for Industry 4.0 and IoT, MetroInd 4.0 and IoT 2020—Proceedings, Roma, Italy, 3–5 June 2020; pp. 526–531. [CrossRef]
25. Patane, F.; Cappa, P. A 3-DOF parallel robot with spherical motion for the rehabilitation and evaluation of balance performance. *IEEE Trans. Neural Syst. Rehabil. Eng.* **2010**, *19*, 157–166. [CrossRef] [PubMed]
26. Taborri, J.; Mileti, I.; Del Prete, Z.; Rossi, S.; Palermo, E. Yaw Postural Perturbation Through Robotic Platform: Aging Effects on Muscle Synergies. In Proceedings of the 2018 7th IEEE International Conference on Biomedical Robotics and Biomechatronics (Biorob), Enschede, The Netherlands, 26–29 August 2018; pp. 916–921. [CrossRef]
27. Mileti, I.; Taborri, J.; Rossi, S.; Del Prete, Z.; Paoloni, M.; Suppa, A.; Palermo, E. Measuring age-related differences in kinematic postural strategies under yaw perturbation. In Proceedings of the 2018 IEEE International Symposium on Medical Measurements and Applications (MeMeA), Rome, Italy, 11–13 June 2018; pp. 1–6. [CrossRef]
28. Bortole, M.; Venkatakrishnan, A.; Zhu, F.; Moreno, J.C.; Francisco, G.E.; Pons, J.L.; Contreras-Vidal, J.L. The H2 robotic exoskeleton for gait rehabilitation after stroke: Early findings from a clinical study. *J. Neuroeng. Rehabil.* **2015**, *12*, 54. [CrossRef] [PubMed]
29. Palermo, E.; Rossi, S.; Marini, F.; Patanè, F.; Cappa, P. Experimental evaluation of accuracy and repeatability of a novel body-to-sensor calibration procedure for inertial sensor-based gait analysis. *Measurement* **2014**, *52*, 145–155. [CrossRef]
30. Cappa, P.; Patanè, F.; Rossi, S.; Petrarca, M.; Castelli, E.; Berthoz, A. Effect of changing visual condition and frequency of horizontal oscillations on postural balance of standing healthy subjects. *Gait Posture* **2008**, *28*, 615–626. [CrossRef] [PubMed]
31. Cicchetti, D.V. Guidelines, Criteria, and Rules of Thumb for Evaluating Normed and Standardized Assessment Instruments in Psychology. *Psychol. Assess.* **1994**, *6*, 284–290. [CrossRef]
32. Zampogna, A.; Mileti, I.; Martelli, F.; Paoloni, M.; Del Prete, Z.; Palermo, E.; Suppa, A. Early balance impairment in Parkinson's Disease: Evidence from Robot-assisted axial rotations. *Clin. Neurophysiol.* **2021**, *132*, 2422–2430. [CrossRef]
33. Grassi, L.; Rossi, S.; Studer, V.; Vasco, G.; Motta, C.; Patanè, F.; Castelli, E.; Rossi, S.; Cappa, P. Quantification of postural stability in minimally disabled multiple sclerosis patients by means of dynamic posturography: An observational study. *J. Neuroeng. Rehabil.* **2017**, *14*, 4. [CrossRef]
34. Blenkinsop, G.M.; Pain, M.T.G.; Hiley, M.J. Balance control strategies during perturbed and unperturbed balance in standing and handstand. *R. Soc. Open Sci.* **2017**, *4*, 161018. [CrossRef]
35. Sung, P.S.; Schalk, B.; Camp, R.; Park, M.S. Gender difference of hip-ankle compensations following a novel trip perturbation in young adults. *Clin. Biomech.* **2020**, *80*, 105194. [CrossRef]

36. Batcir, S.; Shani, G.; Shapiro, A.; Alexander, N.; Melzer, I. The kinematics and strategies of recovery steps during lateral losses of balance in standing at different perturbation magnitudes in older adults with varying history of falls. *BMC Geriatr.* **2020**, *20*, 249. [CrossRef]
37. Chumacero-Polanco, E.; Yang, J. Validation of an ankle-hip model of balance on a balance board via kinematic frequency-content. *Gait Posture* **2020**, *82*, 313–321. [CrossRef] [PubMed]
38. Morasso, P. Centre of pressure versus centre of mass stabilization strategies: The tightrope balancing case. *R. Soc. Open Sci.* **2020**, *7*, 200111. [CrossRef] [PubMed]
39. Fasola, J.; Vouga, T.; Baud, R.; Bleuler, H.; Bouri, M. Balance Control Strategies during Standing in a Locked-Ankle Passive Exoskeleton. *IEEE Int. Conf. Rehabil. Robot.* **2019**, *2019*, 593–598. [CrossRef]
40. Tokur, D.; Grimmer, M.; Seyfarth, A. Review of balance recovery in response to external perturbations during daily activities. *Hum. Mov. Sci.* **2019**, *69*, 102546. [CrossRef] [PubMed]
41. Paillard, T. Cross-Education Related to the Ipsilateral Limb Activity on Monopedal Postural Control of the Contralateral Limb: A Review. *Front. Physiol.* **2020**, *11*, 496. [CrossRef]
42. Mandalidis, D.G.; Karagiannakis, D.N. A comprehensive method for assessing postural control during dynamic balance testing. *MethodsX* **2020**, *7*, 100964. [CrossRef]
43. Keith, T.R.; Condon, T.A.; Phillips, A.; McKeon, P.O.; King, D.L. Postural control strategies are dependent on reach direction in the star excursion balance test. *Int. J. Athl. Ther. Train.* **2016**, *21*, 33–39. [CrossRef]
44. O'Connor, S.M.; Kuo, A.D. Direction-dependent control of balance during walking and standing. *J. Neurophysiol.* **2009**, *102*, 1411–1419. [CrossRef]
45. Shao, Y.; Zhang, W.; Su, Y.; Ding, X. Design and optimisation of load-adaptive actuator with variable stiffness for compact ankle exoskeleton. *Mech. Mach. Theory* **2021**, *161*, 104323. [CrossRef]